

# Bisphosphonate incorporation in surgical implant coatings by fast loading and co-precipitation at low drug concentrations

Jonas Åberg · Ulrika Brohede · Albert Mihranyan ·  
Maria Strømme · Håkan Engqvist

Received: 5 October 2008 / Accepted: 4 May 2009 / Published online: 18 May 2009  
© Springer Science+Business Media, LLC 2009

**Abstract** The objectives of the present work was to evaluate the possibility for fast loading by soaking of bisphosphonates (BPs) into hydroxylapatite (HA) implant coatings biomimetically grown on crystalline TiO<sub>2</sub> surfaces, and also investigate the influence of different BP loading concentrations in a buffer during co-precipitation of a calcium phosphate containing layer onto these surfaces. The co-precipitation method created coatings that contained BPs throughout most of the coating layer, but the presence of BPs in the buffer hindered the formation of a bulk HA-layer, thus resulting in very thin coatings most likely consisting of islands built up by a calcium phosphate containing BPs. The coatings biomimetically grown on TiO<sub>2</sub> surfaces, were shown to consist of crystalline HA. Soaking of these coatings during 15 min only in a low BPs concentration containing buffer yielded a concentration on the coating surface of the same order of magnitude as obtained with soaking during 60 min in significantly higher concentrated buffers. This could be of advantage during surgery since the operating surgeon could make a fast decision whether or not to include the drugs in the coating based on the need of the particular patient at hand. The BPs present on the surface of the fast-loaded HA coatings were found to be strongly bound, something which should be

beneficial for in vivo use. Both the co-precipitation method and the fast loading by soaking method investigated here are promising techniques for loading of BPs onto surgical implants. The simplicity of both methods is an advantage since implants can have spatially complicated structures.

## 1 Introduction

Bisphosphonates (BPs) constitute a class of drugs which has been used since the middle of the 20th century for treatments of bone diseases caused by increased bone resorption such as osteoporosis, Paget's disease and tumor bone diseases [1, 2]. BPs contribute to making the bone structure stronger by increasing the rate of cell death among the osteoclasts [3, 4]. Studies by von Knoch et al. [5] indicate that BPs also have positive effect on the osteoblasts. These properties of BPs have made them interesting for use in connection with bone implants. A more effective bone generation gives a stronger bone structure around the implant which in turn decreases the risk of implant loosening. In animal studies a positive effect from BPs on the bone generation around implants has been observed [6, 7].

BPs can be administered orally or subcutaneously [6]. Both demand higher dose concentrations than locally delivered BPs, which may be achieved by loading BPs into the surface of the implant before implantation [7]. Various loading methods for implant surfaces are suggested of which many rely on the presence of calcium in the surface layer, since BPs have a high affinity to calcium [8]. Calcium ions can either be implanted onto a titanium surface to immobilise BPs on the surface [9], or BPs can be loaded into a Ca containing hydroxylapatite (HA) coating [4, 7,

---

J. Åberg · H. Engqvist (✉)  
Division for Materials Science, Department of Engineering  
Sciences, The Ångström Laboratory, Uppsala University,  
Box 534, 751 21 Uppsala, Sweden  
e-mail: hakan.engqvist@angstrom.uu.se

U. Brohede · A. Mihranyan · M. Strømme (✉)  
Division for Nanotechnology and Functional Materials,  
Department of Engineering Sciences, The Ångström Laboratory,  
Uppsala University, Box 534, 751 21 Uppsala, Sweden  
e-mail: maria.stromme@angstrom.uu.se

10–12]. Seshima et al. used granules of HA and studied the loading of BPs into—and the subsequent release from—these granules [13]. In these studies [4, 7, 10–13] the loading was performed by soaking the samples in a solution of BPs dissolved in water.

When a bioactive surface is soaked in simulated body fluid (SBF) a HA coating is formed on the surface from the constituents of the SBF; a similar coating can be obtained when a bioactive surface is soaked in phosphate buffer saline (PBS) [14–17]. Attempts to load the HA layer with BPs have been made, both by soaking into the HA layer and by co-precipitation onto the surface [4]. Mcleod et al. [4] compared water with SBF as a dissolution media for BPs. In their study they observed a higher BP content in samples soaked in SBF than in samples soaked in water, when analysed with Electron Spectroscopy for Chemical Analysis (ESCA; also frequently referred to as X-Ray Photoelectron Spectroscopy). From this they drew the conclusion that BPs were precipitated simultaneously with HA on surfaces of samples soaked in SBF, not only adsorbed onto the surface. Cell culture studies revealed that the effect on osteoclasts was the same for both samples [4]. To form a biomimetic HA layer into which pharmaceutically active ingredients can be loaded may be difficult, especially on metals and polymers. Normally this is done via chemical treatment of the surface or extensive soaking times. An alternative method, which also creates a potentially beneficial long term surface, is to coat the implant with a more bioactive surface chemistry, i.e. a bioactive surface like calcium phosphate, crystalline titanium oxide or the like [18–20].

Since HA on implants is resorbed after implantation, inclusion of BPs in HA may allow for a continuous local administration of BPs until full bone ingrowth has been completed, giving a strong bone structure around the implant. To optimize this process, the BPs should preferably be strongly bound to the HA layer. It has been proposed that Pamidronate disodium hydrate, which is a nitrogen containing BP, can diffuse at least 250 nm into plasma sprayed HA coatings [11], that normally have a thickness in the range of 30–200  $\mu\text{m}$  [21]. If the Pamidronate could be included in the HA structure at the same time as the HA layer is formed a continuous long-term administration would be assured.

The main drawback of this type of implant surface is that it reduces the liberty for the surgeon dealing with the implant. If the implant already contains BPs the surgeon will not have the option to include or exclude the drug based on the patient need. In some cases the risk of infection is large so instead of BPs antibiotics are needed [20] or even a combination of drugs. Therefore, to increase the range of options for the clinician and also to facilitate implant manufacturing and sterilization, a method allowing

the implant to be quickly loaded with drugs in a procedure that can be carried out during or immediately before surgery, would be very valuable. In addition this may simplify the regulatory approval of the implant since the implant and the drug may be regulated separately.

In the present work we evaluate the possibility for fast loading by soaking of Pamidronate into HA coatings biomimetically grown on crystalline  $\text{TiO}_2$  surfaces, and also investigate the influence of different Pamidronate loading concentrations in a PBS buffer during co-precipitation of a calcium phosphate containing layer onto these surfaces.

## 2 Experimental

### 2.1 Sample preparation

Gradient titanium dioxide thin films were deposited on  $20 \times 20$  mm plates of commercially pure grade 5 titanium by physical vapour deposition (PVD). The gradient coating, tailored to optimize the adhesion of the coating to the substrate [19], was prepared in a reactive dc magnetron-sputtering unit (Balzer UTT400). The working chamber was mounted with a turbo molecular pump TMU 521P.

The chamber base pressure was  $\sim 10^{-7}$  mbar after backing. Pure titanium (99.9%) was used as target. Pure argon (99.997%) and oxygen (99.997%) were used for the reactive sputtering. The substrate was kept at a constant temperature of 350°C during the entire process.

The oxygen profile of the film was controlled by changing the oxygen flow. A crystalline titanium dioxide was ensured by heat treatment of the sputtered film at 385°C in air for one hour post deposition. The targeted coating design parameters were as follows, described from the titanium substrate; 50 nm of pure titanium, 50 nm gradually increasing oxygen content from Ti to  $\text{TiO}_2$  and a top layer of 100 nm crystalline  $\text{TiO}_2$ .

The thickness of the films was measured with surface profilometry, using a Tencor Alpha-step 200 instrument (USA product).

After the heat treatment the samples were ultrasonically cleaned, at resonance of 20 kHz, by the following procedure; 5 min in 100 ml of acetone then 5 min in ethanol and finally 5 min in deionized water.

### 2.2 Loading of pamidronate

Two methods were employed to obtain BPs containing coatings on the sputter deposited  $\text{TiO}_2$  surfaces; co-precipitation directly onto the surfaces and fast loading by soaking into a biomimetically grown HA layer on the same surfaces. The bisphosphonate used was Pamidronate disodium salt hydrate,  $\text{C}_3\text{H}_9\text{NO}_7\text{P}_2\text{Na}_2 \cdot x\text{H}_2\text{O}$ , (Sigma Aldrich, 95%).

### 2.2.1 Co-precipitation directly onto the TiO<sub>2</sub> surface

Pamidronate was dissolved in 10 ml of PBS (Dulbecco, containing CaCl<sub>2</sub>, MgCl<sub>2</sub>, KCl, KH<sub>2</sub>PO<sub>4</sub>, NaCl and Na<sub>2</sub>HPO<sub>4</sub>, Sigma-Aldrich) in a test tube with a conical bottom. Four different concentrations were used, see Table 1. The TiO<sub>2</sub> covered samples were stored in the buffer for seven days at 40°C after which the samples were removed from the buffer, gently rinsed in distilled water and air dried.

### 2.2.2 Fast loading by soaking into biomimetically grown HA

The TiO<sub>2</sub> covered samples were soaked in 10 ml of PBS for seven days at 40°C to allow for a homogenous HA layer to form on the surface (samples HA-Ref). Next the samples were removed from the buffer, gently rinsed in distilled water and air dried. Thereafter some of the samples were soaked in 10 ml of a solution of Pamidronate in deionized water (0.5 mg/ml) for 15 min (samples S15) or 60 min (samples S60). After soaking, the samples were air dried.

Pamidronate containing reference samples (samples Pam) were prepared by depositing an aqueous solution of Pamidronate (10 mg/ml) directly on TiO<sub>2</sub> covered samples. Thereafter the samples were placed in 40°C until the water had evaporated.

## 2.3 Analysis

### 2.3.1 ESCA

A full elemental analysis of the surface and an element specific analysis of the bulk of the coating were done by ESCA using a Physical Electronics Quantum 2000 spectrometer with monochromatic Al K  $\alpha$  radiation. The diameter of the area of analysis was set to 100  $\mu$ m. Pass energy was set to 187.85 eV and a step size of 0.8 eV was used. The same settings were used for both the surface analysis and the depth profile. Depth profiles were obtained using Ar<sup>+</sup>-ion sputtering over an area of 4  $\times$  4 mm<sup>2</sup>. The

energy of the incident ions was 2 keV unless otherwise stated. Spectra were acquired for the following peaks; C1s, Ca2p, N1s, O1s, P2p and Ti2p after each sputter cycle of 0.2 min. Nitrogen and carbon were used as indicators for presence of Pamidronate since these are the only two elements that are present in Pamidronate but not in HA. With these sputtering parameters the sputtering rate was estimated to 7.5 nm per minute [4], based on sputter rates on HA reported in literature [4, 22]. The positions in energy of the ESCA peaks were shifted with respect to that of oxygen 1 s at 531 eV to minimize errors due to charging of the surface during analysis.

### 2.3.2 X-ray diffraction (XRD)

To investigate if crystalline HA was present on the sample surfaces, both the soaked and the co-precipitated samples were analysed using XRD. The XRD measurements were performed using a Siemens D5000 diffractometer. The grazing incidence angle was 0.2° in parallel beam geometry using CuK $\alpha$  radiation (wavelength 1.540598 Å). Collection of diffracted X-rays was done between 20° and 42° 2 $\theta$  for 2 s every 0.2°.

### 2.3.3 Scanning electron microscopy (SEM)

The surface structure of the samples was examined with SEM using a LEO 1550 equipped with a field emission gun. An inlens detector was used and the acceleration voltage was set to 3.35 kV. During SEM analysis energy dispersive X-ray analysis (EDX) was performed for element analysis.

### 2.3.4 Alternating ionic current (AIC) conductivity measurements

The AIC technique is a method developed to measure release of ionic drugs from a host [23, 24]. Since Pamidronate is ionic AIC was used to detect its release. The samples were placed in the AIC-cell and immersed in 20 ml of distilled water. A small magnet stirrer was used to ensure a uniform distribution of ions in the liquid. Measurements were performed during 24 h.

**Table 1** Pamidronate concentrations used in co-precipitation experiments

Sample name	Concentration (mg/ml)
Co-P 0.5	0.5
Co-P 0.1	0.1
Co-P 0.02	0.02
Co-P 0.004	0.004

## 3 Results and discussion

### 3.1 Coatings made by co-precipitation

#### 3.1.1 ESCA surface analysis

The concentration of elements on the surface of all samples presented in Table 1 as well as of the Pamidronate (Pam)

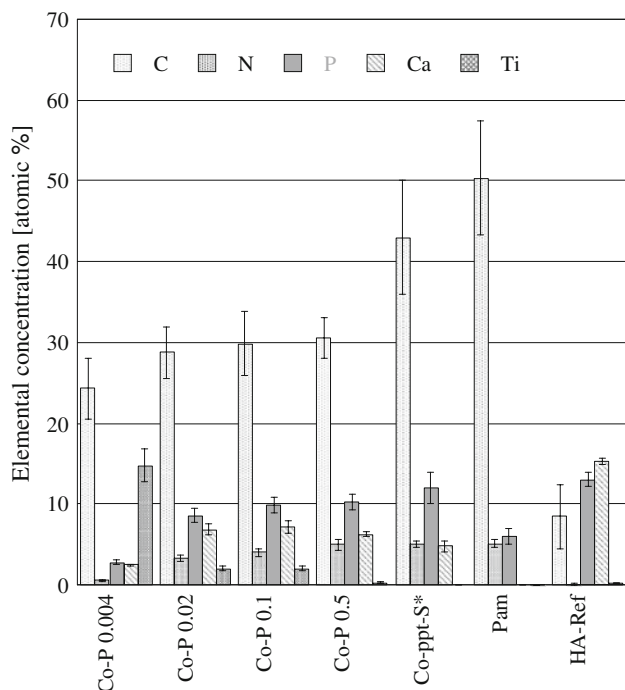


**Fig. 1** Concentration of elements on sample surfaces prepared with co-precipitation in solution containing Pamidronate and PBS. The results for the Co-ppt-S sample is taken from the literature [4]. The numbers following the samples names Co-P indicate the Pamidronate concentration in mg/ml used in the co-precipitation procedure. The values are average values after measurements made on two samples and the error bars denote the absolute deviation of these experiments

and the HA (HA-Ref) reference samples is shown in Fig. 1, together with the results from previous research [4]. From the nitrogen content in the samples it could be deduced that Pamidronate was present in all coatings that had been made by co-precipitation in a Pamidronate containing buffer. The presence of calcium and phosphorous on all sample surfaces also indicates that calcium phosphate crystals were formed during storage in the buffer.

The theoretical maximum nitrogen content—calculated from the chemical formula of a dehydrated Pamidronate salt—is 6.7% for a surface completely covered with Pamidronate, not counting the hydrogen atoms since these are not detected in the ESCA experiments. However as seen in Fig. 1, the concentration of nitrogen on the Pamidronate reference (Pam) was only  $5.1 \pm 0.5\%$ . Since Pamidronate has a high affinity to calcium and is expected to form calcium pamidronate when co-precipitated, the maximum amount of Pamidronate that can adsorb will be limited by the number of  $\text{Ca}^{2+}$  ions available, about which the phosphate anions are also competing. As will become clear from the analysis of the depth profiles presented below, calcium binds to the  $\text{TiO}_2$  surface before phosphorous and Pamidronate are adsorbed. Thus, the number of available  $\text{Ca}^{2+}$  ions, as well as the Pamidronate surface

concentration is expected to be proportional to the surface area of the  $\text{TiO}_2$  substrate.

When looking closer at the nitrogen content of the different Co-P sample surfaces and of the literature [4] Co-ppt-S sample, it becomes clear that a lower Pamidronate concentration in the PBS buffer used in the co-precipitation gave lower Pamidronate content on the sample surface. The concentration of nitrogen on the analysed sample surface as a function of Pamidronate concentration in the PBS buffer is plotted in Fig. 2. For the lowest concentration used there were only small amounts of Pamidronate loaded onto the surface. For Pamidronate buffer concentrations above 0.004 mg/ml, the rise in nitrogen sample surface concentration was rapid up to a buffer concentration of  $\sim 0.5$  mg/ml for which the nitrogen concentration curve seem to level out to give a constant nitrogen content of around 5%. Clearly, with a Pamidronate concentration of only 0.5 mg/ml in PBS almost the same concentration of Pamidronate on the surface of the co-precipitated coatings could be achieved as by McLeod et al. [4] employing a six times higher Pamidronate buffer concentration. As previously discussed, the amount of Pamidronate adsorbed is not only expected to be a function of the amount of Pamidronate in the buffer solution but also of the number of  $\text{Ca}^{2+}$  ions adsorbed to the substrate, and thus also of the substrate surface area.

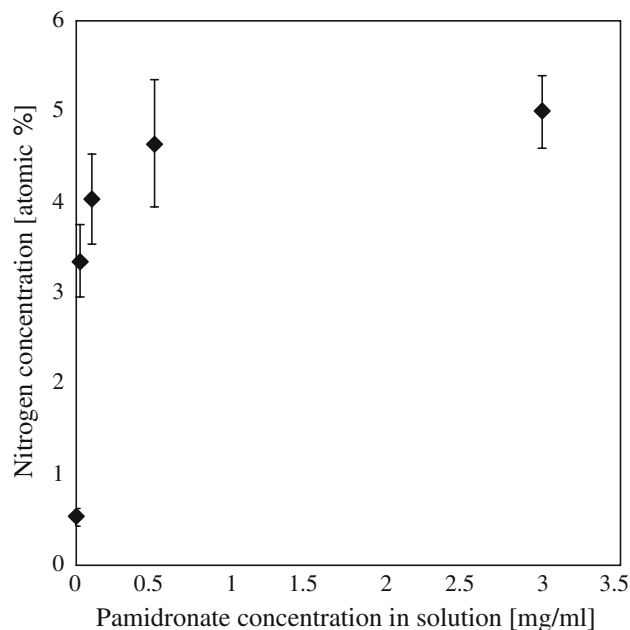


**Fig. 2** Relation between the nitrogen concentration on sample surface and the Pamidronate concentration in the PBS buffer. The values are average values after measurements made on two samples and the error bars denote the absolute deviation of these experiments. The 3 mg/ml value corresponds to the Co-ppt-S sample from Ref. [4] for which the error bars represents the standard deviation with  $n = 3$

Also the levels of carbon and phosphorous in the coatings were lower for lower Pamidronate buffer concentrations. Carbon is a common constituent of most contaminations so it can not be used to indicate Pamidronate by it self. Nevertheless, it is likely that the lower carbon concentrations were caused by a lower Pamidronate content. Phosphorous is in this case not the best indicator of Pamidronate either since calcium phosphates and HA also contain phosphorous. However, in HA (HA-Ref) there is more calcium than phosphorous which is seen in Fig. 1. This was not the case for the samples prepared in Pamidronate containing buffers. So the additional amount of phosphorous seen in Fig. 1 in the Co-P samples further indicates the presence of Pamidronate on the surface.

An increasing amount of titanium with decreasing Pamidronate buffer concentrations was detected on the surface of the co-precipitated samples that had been prepared in buffers containing less than or equal to 0.1 mg/ml Pamidronate, see Fig. 1. On the Co-P 0.5 sample surface the amount of titanium was found to be below the detection limit of the instrument. These findings indicate that the co-precipitated coatings, created by storage in the low Pamidronate concentration buffers, contain regions with a thickness of 3–5 nm or less (3–5 nm is the analysis depth of ESCA [25, 26]). The layer thickness of the coatings formed in a 0.5 mg/ml Pamidronate containing buffer under the experimental conditions used here is larger than this value.

### 3.1.2 SEM and XRD surface analysis

No continuous layer with the morphology typical for crystalline HA could be observed in the SEM analysis of the co-precipitated samples. Instead, a coating seemingly consisting of small protrusions, not typical for TiO<sub>2</sub> or HA, was visible, see Fig. 3. The XRD diffractograms confirmed the absence of crystalline structures on the surfaces, while the EDX analysis confirmed the results from the ESCA analysis showing on the presence of calcium and

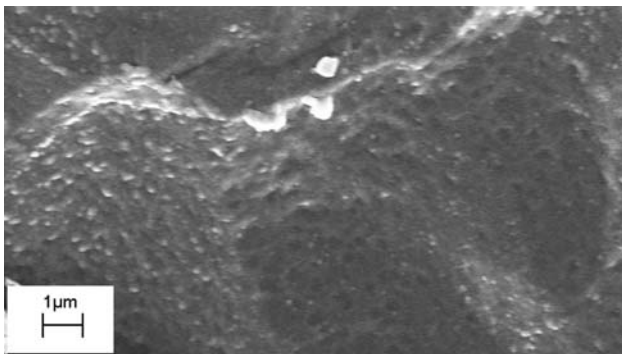


**Fig. 3** SEM image of the surface of a Co-P 0.5 sample

phosphorous. In order to obtain more information about the elemental content of the co-precipitated coating and about its thickness, ESCA depth profiles were recorded.

### 3.1.3 ESCA depth profiles

Figure 4 shows the atomic concentration in the bulk of the sample coatings as a function of the distance from the surface. To simplify the interpretation of the profiles the oxygen concentration curves have been left out in all figure panels. In all samples, the oxygen concentration remained at 60–65% throughout the profile. Minor contamination of the sample surfaces is difficult to avoid, something which results in a high carbon content at the surface. After a few sputter cycles, however, most of the contamination was removed. In all samples the carbon content decreased rapidly during the first couple of sputter cycles after which it followed the trend of the nitrogen content, thus indicating that the carbon detected deeper into the surface was present in the Pamidronate.

By observing the titanium content as well as the nitrogen content in the profiles the thickness of the coating can be estimated. When the concentration of titanium reaches 33%, the TiO<sub>2</sub> covered substrate has been reached. Likewise, when the nitrogen content reaches zero no Pamidronate containing coating exists. The exact thickness of the coating is not possible to establish since the thickness was probably not homogenous all over the surface, as indicated by the SEM images, and the TiO<sub>2</sub> covered substrate was not perfectly smooth. The elemental content of the surface represents an average value over a circular area of 100 μm in diameter, which was the dimension of the analysis regions in the ESCA experiments. For the co-precipitated samples prepared in buffers containing 0.1 mg/ml Pamidronate or less, the ESCA profiles (Fig. 4b–d) show that some titanium is present on the surface, whereas a titanium concentration of around 30% is not found before a sputtering depth of ~8, ~30, and ~45 nm has been reached for Co-P 0.004, Co-P 0.02, and Co-P 0.1, respectively. At approximately the same depths the nitrogen content approaches zero. This together with the behaviour of the calcium and phosphorous profiles and the SEM images can be taken as evidence for a coating that is not homogeneously covering the surface but that is built up by islands, consisting of Pamidronate containing calcium phosphate, that grow larger and thicker as the Pamidronate content in the buffer is increased. For the Co-P 0.5 sample no titanium was detected on the surface illustrating that the above mentioned islands most likely are linked together in this sample. The presence of titanium at a depth of only 5 nm (Fig. 4a) and the fact that only ~25% titanium is found at a sputtering depth of 45 nm, indicates that the islands start to merge as the Pamidronate content of the



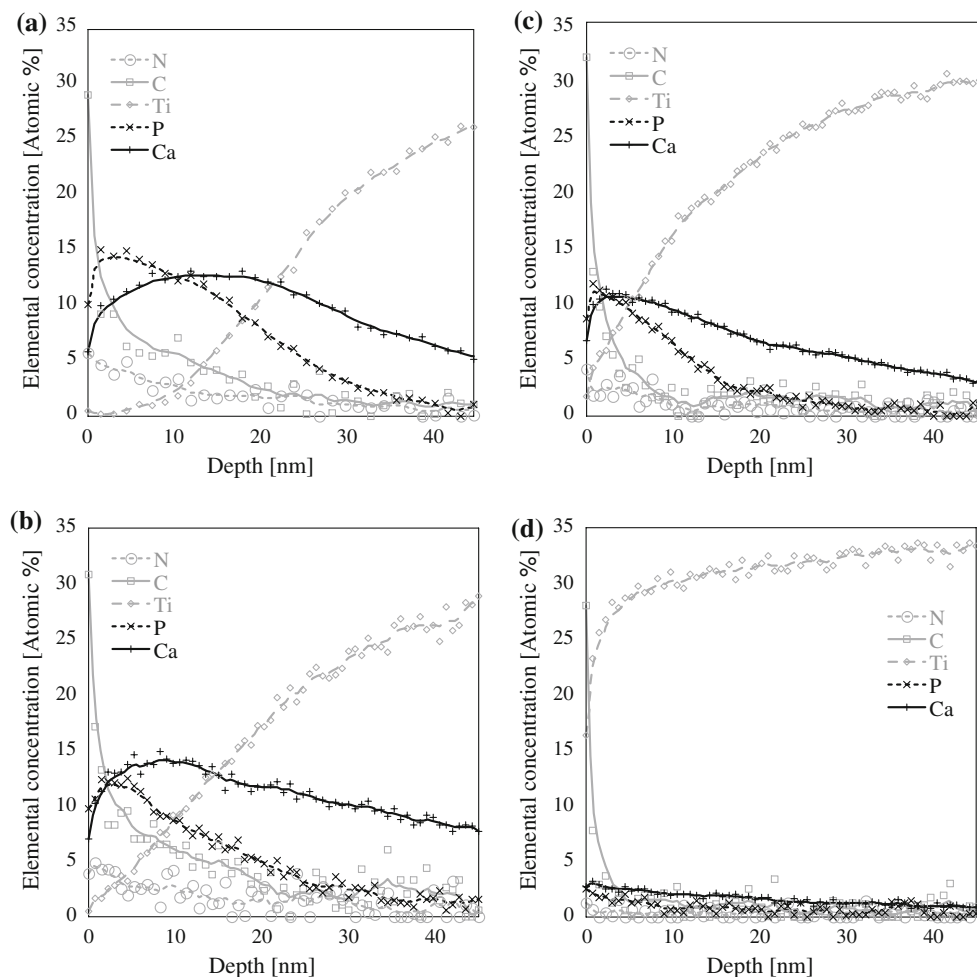


**Fig. 4** ESCA depth profile of **a** Co-P 0.5, **b** Co-P 0.1, **c** Co-P 0.02, **d** Co-P 0.004

buffer is high enough. The fluctuations in both the nitrogen and carbon concentration curve that can be observed deeper than  $\sim 10$  nm into the studied coatings are probably caused by sputtered material that has deposited close to the analysed area and hence might influence the detection.

A thorough comparison of the nitrogen, calcium and phosphorous depth profiles shows that in all samples calcium and phosphorous were located slightly deeper into the coating than the nitrogen of Pamidronate, thus indicating that the formation of calcium phosphate occurs right before Pamidronate is adsorbed. Noteworthy is also that calcium was always detected somewhat deeper into the material than phosphorous. Both the Pamidronate and the phosphate ions bind to calcium. Conceivably the smaller size of the phosphate ions and the fact that the concentration of phosphate ions is higher than the concentration of Pamidronate in the buffer result in a faster adhesion of phosphate than Pamidronate to calcium, which would explain the profiles. The observed behaviour is coherent with the theory of formation of HA as described by Yang et al. [27] although

our results did not show on the presence of a HA layer. The very thin coatings formed in the co-precipitation experiments correspond well to results of previous work in which bisphosphonates have been proven to restrain the formation of calcium phosphate crystals [8]. Having established that the coating does not consist of crystalline HA, the results showing that a higher Pamidronate concentration yields a thicker coating indicate that a different calcium phosphate phase is formed in the presence of Pamidronate. A more thorough evaluation of the structure and chemistry of this phase could possibly be achieved by transmission electron microscopy and high resolution ESCA.

### 3.2 Coatings fast loaded by BPs

#### 3.2.1 Surface analysis by ESCA, SEM and XRD

In Fig. 5 the concentrations of elements measured with ESCA on the surface of samples prepared using the fast loading method is shown together with results from

previously published experiments [4]. The results for the reference HA sample (HA-Ref) is also included in the figure. As expected, nitrogen was present on the surface of all samples that had been soaked in a Pamidronate containing buffer. The HA reference sample contained amounts of nitrogen that are below the limit of detection of the instrument. 15 min of soaking yielded a nitrogen content of  $1.1 \pm 0.1\%$  on the coating surface which was only slightly less than the  $1.3 \pm 0.1\%$  nitrogen detected in the sample soaked for 60 min. The results from previous experiments [4] of soaking during 60 min rendered somewhat higher amounts of Pamidronate ( $2.4 \pm 0.3\%$ ) on the surface. The latter experiment was performed using a pamidronate concentration six times higher which explains the difference.

The atomic percentage of carbon and phosphorous followed the same trend as nitrogen. On samples soaked in a Pamidronate containing buffer there was more phosphorous than calcium; on the HA-Ref surface the situation was the opposite.

When comparing the results in Fig. 5 to the results from the co-precipitated samples in Fig. 1 it is clear that more Pamidronate is present on the surface of samples prepared with the co-precipitation method. As it was shown by Peter et al. [12], however, a higher concentration of bisphosphonate in the implant surface does not necessarily give better

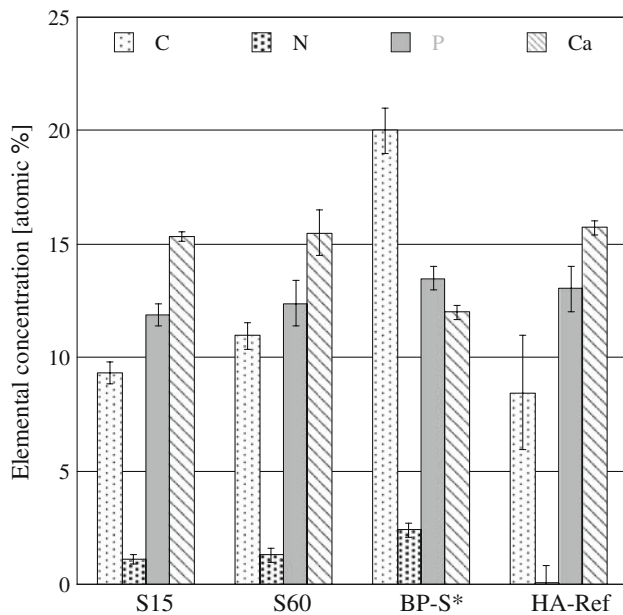


**Fig. 5** Concentration of elements on sample surfaces of biomimetically deposited HA coating soaked in Pamidronate containing PBS buffer. The numbers following the samples names S indicate the time in minutes the samples were soaked. The values are average values after measurements made on two samples and the error bars denote the absolute deviation of these experiments. The results for the BP-S sample is taken from the literature [4] for which the error bars represents the standard deviation with  $n = 3$

results in vivo. As well, the co-precipitated coatings were very thin and clearly not built up by crystalline HA. In the fast loading by soaking experiments, the surface was homogenously covered with a layer of HA crystals which was formed during the soaking in PBS as evident from the SEM image of a S60 sample surface in Fig. 6. Similar structures were observed on the S15 and HA-Ref samples as well. XRD analysis of the samples showed the presence of HA as seen in the inset of Fig. 6; the peaks at  $26^\circ$  and  $32^\circ$  are characteristic for HA [28].

The ESCA depth profiles of the soaked samples S15 and S60 did not show presence of Pamidronate in the bulk of the coatings, whereas in Ref. [11] it was reported that Pamidronate had diffused into the bulk of the plasma sprayed HA coatings. This could be explained by the difference in microstructure between biomimetic and plasma sprayed HA coatings [29]. Plasma spraying gives a denser structure (less pore volume), which often contains some deeper micro pores. When a plasma sprayed sample is soaked in a Pamidronate containing buffer, the buffer fills these pores and Pamidronate can attach to the walls of the pores. In an ESCA analysis of such a sample one, thus, finds Pamidronate at different distances from the top surface even if there is no Pamidronate diffusion into the bulk of the coating. Biomimetic coatings on the other hand becomes more porous (higher pore volume) but without the deep micropores present in the plasma sprayed coatings. Hence, in such coatings one is only expected to find Pamidronate in the top surface of the coating.

Even when a higher sputtering voltage of 4 kV was applied in the ESCA analysis of the HA coatings used in the fast-loading experiments, the layer was not penetrated indicating that the thickness of the coatings was larger than 100 nm. In general the HA coatings described in the literature are several microns thick but it has been shown that

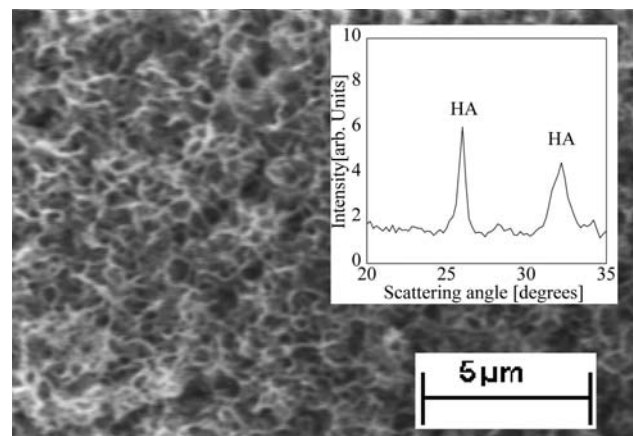


**Fig. 6** SEM image of HA crystals on an S60 sample. The inset shows an XRD spectrum of the sample

substantially thinner coatings can enhance the bone formation in vivo [30].

### 3.2.2 Release of BPs studied by AIC conductivity measurements

To investigate if Pamidronate is released from the fast-loaded coatings, measurements were made with the AIC method. In Fig. 7 the conductance curves of S60 and HA-Ref samples are depicted. Overall, the measured conductance in the solution surrounding both samples was extremely low showing that the total amount of ions released from the coatings was minute. The curves closely follow each other indicating that there was no significant difference in the amount of released ions from the surface of the two samples. After ~10 h the curves slightly separate, but as seen in the figure the maximum difference between them is less than the conductance level at time zero signifying the conductivity of deionised water. From this we can conclude that the Pamidronate present in the fast-loaded samples is strongly bound to the HA structure, in good correspondence with previous studies [10]. Hence, even if the Pamidronate of these samples are present in the outermost surface layer of the coating only, an in vivo action of the Pamidronate for as long as it takes for the surface layer of HA to resorb is expected: The HA dissolution is expected to be slowed down significantly by the presence of Pamidronate on the surface since the drug inhibits osteoclast formation. This should allow the osteoblasts to form a dense bone structure around the implant giving a strong ingrowth of bone at the implant surface.

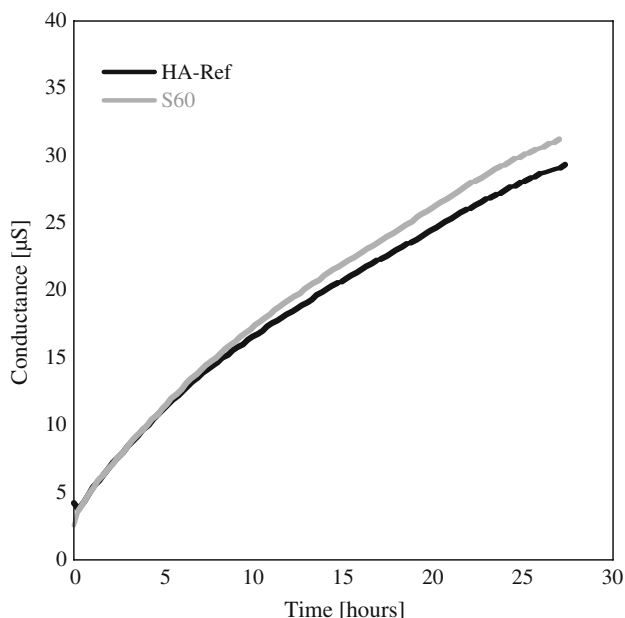


**Fig. 7** Conductance of solution surrounding an S60 and a HA-Ref sample in the AIC experiment

## 4 Conclusions

The possibility of fast loading by soaking of Pamidronate, which is a nitrogen containing bisphosphonate, into biomimetic HA coatings grown on sputter deposited crystalline TiO<sub>2</sub> surfaces has been evaluated. As well, the influence of different Pamidronate loading concentrations in a PBS buffer during co-precipitation of a calcium phosphate containing layer onto these surfaces has been studied.

It was found that both methods yielded Pamidronate containing coatings. The co-precipitation method created coatings that contained Pamidronate throughout most of the coating layer. However, the presence of Pamidronate in the PBS buffer was shown to hinder the formation of a bulk HA-layer of the type formed when Pamidronate was absent in the buffer, thus resulting in very thin coatings most likely consisting of islands built up by a calcium phosphate containing Pamidronate.

The biomimetic coatings grown on TiO<sub>2</sub> surfaces in a PBS, were shown to consist of crystalline HA. It was further shown that soaking of these coatings during 15 min in a low Pamidronate concentration containing buffer yielded a concentration on the coating surface of the same order of magnitude as obtained with soaking during 60 min in significantly higher concentrated buffers. This could be of advantage during surgery since the operating surgeon could make a fast decision whether or not to include the drugs in the coating based on the need of the particular patient at hand. As well there is a cost advantage in using low concentrations of bisphosphonates, since bisphosphonates are expensive drugs [31]. The Pamidronate present on the surface of the fast-loaded HA coatings were found to be strongly bound something which should be beneficial for in vivo use.

Both the co-precipitation method and the fast loading by soaking method investigated are promising techniques for loading of bisphosphonates onto implants. The simplicity of both methods is an advantage since implants can have spatially complicated structures.

**Acknowledgement** The author greatly acknowledges The Swedish Governmental Agency for Innovation Systems (VINNOVA) and The Swedish Research Council (VR) for financial support.

## References

- Francis MD, Valent DJ. Historical perspectives on the clinical development of bisphosphonates in the treatment of bone diseases. *J Musculoskelet Neuronal Interact.* 2007;7:2–8.
- Fleisch H. The role of bisphosphonates in breast cancer: development of bisphosphonates. *Breast Cancer Res.* 2002;4:30–4. doi: 10.1186/bcr414.



3. Ito M, et al. Ultrastructural and cytochemical studies on cell death of osteoclasts induced by bisphosphonate treatment. *Bone*. 1999;25:447–52. doi:10.1016/S8756-3282(99)00197-0.
4. McLeod K, et al. Adsorption of bisphosphonate onto hydroxyapatite using a novel co-precipitation technique for bone growth enhancement. *J Biomed Mater Res A*. 2006;79A:271–81. doi:10.1002/jbm.a.30792.
5. Knoch F, et al. Effects of bisphosphonates on proliferation and osteoblast differentiation of human bone marrow stromal cells. *Biomaterials*. 2005;26:6941–9. doi:10.1016/j.biomaterials.2005.04.059.
6. Eberhardt C, et al. The bisphosphonate ibandronate accelerates osseointegration of hydroxyapatite-coated cementless implants in an animal model. *J Orthop Sci*. 2007;12:61–6. doi:10.1007/s00776-006-1081-2.
7. Peter B, et al. Local delivery of bisphosphonate from coated orthopedic implants increases implants mechanical stability in osteoporotic rats. *J Biomed Mater Res A*. 2006;76A:133–43. doi:10.1002/jbm.a.30456.
8. Fleisch H. Bisphosphonates: mechanisms of action. *Endocr Rev*. 1998;19:80–100. doi:10.1210/er.19.1.80.
9. Kajiwara H, et al. The bisphosphonate pamidronate on the surface of titanium stimulates bone formation around tibial implants in rats. *Biomaterials*. 2005;26:581–7. doi:10.1016/j.biomaterials.2004.02.072.
10. Yoshinari M, et al. Immobilization of bisphosphonates on surface modified titanium. *Biomaterials*. 2001;22:709–15. doi:10.1016/S0142-9612(00)00234-9.
11. McLeod K, et al. XPS and bioactivity study of the bisphosphonate pamidronate adsorbed onto plasma sprayed hydroxyapatite coatings. *Appl Surf Sci*. 2006;253:2644–51. doi:10.1016/j.apsusc.2006.05.031.
12. Peter B, et al. Calcium phosphate drug delivery system: influence of local zoledronate release on bone implant osteointegration. *Bone*. 2005;36:52–60. doi:10.1016/j.bone.2004.10.004.
13. Seshima H, et al. Control of bisphosphonate release using hydroxyapatite granules. *J Biomed Mater Res B Appl Biomater*. 2006;78B:215–21. doi:10.1002/jbm.b.30446.
14. Kokubo T, Takadama H. How useful is SBF in predicting in vivo bone bioactivity? *Biomaterials*. 2006;27:2907–15. doi:10.1016/j.biomaterials.2006.01.017.
15. Ma J, et al. Biomimetic processing of nanocrystallite bioactive apatite coating on titanium. *Nanotechnology*. 2003;14:619–23. doi:10.1088/0957-4484/14/6/310.
16. Stigter M, et al. Incorporation of tobramycin into biomimetic hydroxyapatite coating on titanium. *Biomaterials*. 2002;23:4143–53. doi:10.1016/S0142-9612(02)00157-6.
17. Mhryan A, et al. A study of the specific surface area evolution during biomimetic growth of hydroxyapatite. *Langmuir*. 2009;25:1292–5. doi:10.1021/la803520k.
18. Wang X, et al. Apatite deposition on thermally and anodically oxidized titanium surfaces in a simulated body fluid. *Biomaterials*. 2003;24:4631–7. doi:10.1016/S0142-9612(03)00357-0.
19. Brohede U, et al. A novel graded bioactive coating on implant for enhanced fixation to bone. *Appl Surf Sci*. 2009; in press. doi:10.1016/j.apsusc.2009.04.149.
20. Brohede U, et al. Multifunctional implant coatings providing possibilities for fast antibiotics loading with subsequent slow release. *J Mater Sci Mater Med*. 2009; in press. doi:10.1007/s10856-009-3749-6.
21. Yang YZ, et al. Review on calcium phosphate coatings produced using a sputtering process—an alternative to plasma spraying. *Biomaterials*. 2005;26:327–37. doi:10.1016/j.biomaterials.2004.02.029.
22. Miller RG, et al. Auger electron spectroscopy of dentin: elemental quantification and the effects of electron and ion bombardment. *Dent Mater*. 1993;9:280–5. doi:10.1016/0109-5641(93)90075-2.
23. Frenning G, et al. A new method for characterizing the release of drugs from tablets in low liquid surroundings. *J Pharm Sci*. 2002;91:776–84. doi:10.1002/jps.10077.
24. Garcia-Bennett AE, et al. A mechanistic study of the formation of mesoporous structures from in situ ac conductivity measurements. *Langmuir*. 2007;23:9875–81. doi:10.1021/la700899s.
25. [http://www.eaglabs.com/techniques/analytical\\_techniques/xps\\_esca.php](http://www.eaglabs.com/techniques/analytical_techniques/xps_esca.php). Accessed 12 may 2008.
26. <http://www.probion.fr/xps.php>. Accessed 12 may 2008.
27. Yang Z, et al. Mechanism and kinetics of apatite formation on nanocrystalline TiO<sub>2</sub> coatings: a quartz crystal microbalance study. *Acta Biomater*. 2008;4:560–8. doi:10.1016/j.actbio.2007.10.003.
28. Ciobanua G, Carjaa G. Structural characterization of hydroxyapatitenext term layer coatings on titanium supports. *Surf Coat Tech*. 2008;202:2467–70. doi:10.1016/j.surfcoat.2007.11.038.
29. Sampathkumaran U, et al. Hydroxyapatite coatings on titanium. *Adv Eng Mater*. 2001;3(6):401–5. doi:10.1002/1527-2648(200106)3:6<401::AID-ADEM401>3.0.CO;2-L.
30. Mohammadi S, et al. Long-term bone response to titanium implants coated with thin radiofrequency magnetron-sputtered hydroxyapatite in rabbits. *Int J Oral Max Impl*. 2004;19:498–509.
31. Hillner BE, et al. Pamidronate in prevention of bone complications in metastatic breast cancer: a cost-effectiveness analysis. *J Clin Oncol*. 2000;18:72–9.